Biosensors and Bioelectronics 24 (2008) 566–571

Contents lists available at ScienceDirect

Biosensors and Bioelectronics

journal homepage: www.elsevier.com/locate/bios

# A novel hydrogen peroxide biosensor based on the immobilization of horseradish peroxidase onto Au-modified titanium dioxide nanotube arrays

A.K.M. Kafi, Guosheng Wu, Aicheng Chen*

*Department of Chemistry, Lakehead University, 955 Oliver Road, Thunder Bay, Ontario P7B 5E1, Canada*

ARTICLE INFO

*Article history:*
Received 14 March 2008
Received in revised form 3 May 2008
Accepted 4 June 2008
Available online 12 June 2008

*Keywords:*
Au-modified titania nanotube arrays
HRP
Biosensors
Hydrogen peroxide
Methylene blue

ABSTRACT

In this study, we report on a promising $H_2O_2$ biosensor based on the co-immobilization of horseradish peroxidase (HRP) and chitosan onto Au-modified $TiO_2$ nanotube arrays. The titania nanotube arrays were directly grown on a Ti substrate using anodic oxidation first; a gold thin film was then uniformly coated onto the $TiO_2$ nanotube arrays by an argon plasma technique. The morphology and composition of the fabricated Au-modified $TiO_2$ nanotube arrays were characterized by scanning electron microscopy (SEM) and energy-dispersive X-ray spectroscopy (EDS). Cyclic voltammetry and chronoamperometry were used to study and to optimize the performance of the resulting electrochemical biosensor. The effect of pH, applied electrode potential, the presence of the electron-mediator methylene blue, and the anodic oxidation time of the Ti substrate on the electrochemical biosensor has been systemically studied. Our electrochemical measurements show that the Au-modified $TiO_2$ nanotube arrays provide excellent matrices for the immobilization of HRP and that the optimized electrochemical biosensor exhibits long linearity, a low detection limit, high stability and very good reproducibility for the detection of $H_2O_2$. Under the optimized conditions the linearity of the developed biosensor for the detection of $H_2O_2$ is observed from $5 \times 10^{-6}$ to $4 \times 10^{-4}$ mol $l^{-1}$ with a detection limit of $2 \times 10^{-6}$ mol $l^{-1}$ (based on the S/N = 3).



## 1. Introduction

Since Clark and Lyons (1962) first introduced the biosensor conception, in which an enzyme is integrated on an electrode surface to build up a biosensor, there has been growing interest in this field. The development of biosensors, particularly in terms of sensitivity, selectivity, stability and simplicity has made significant progress (Kim et al., 2008; Jia et al., 2008). The sensitive and accurate detection of hydrogen peroxide ($H_2O_2$) is of great interest to researchers because of its importance in the pharmaceutical, clinical and industrial settings (Wang and Wang, 2004). Several techniques have been proposed for the detection of $H_2O_2$. Among them, flourometry (Li and Dasgupta, 2000), spectrophotometry (Matsubara et al., 1992), chemiluminescence (Nakashima et al., 1991), titremetry (Hurdis, 1954) and electrochemical biosensors (Ferapontova et al., 2001; Sun et al., 2007; Zhang and Li, 2004; Shumyantseva et al., 2004) have been widely explored. It is very important to consider both response time and cost when fabricating a biosensor. The techniques mentioned above, except for the electrochemical biosensor, involve high cost and are time consuming. Because of their simplicity and high selectivity and sensitivity, electrochemical techniques have been extensively employed for the design of a $H_2O_2$ biosensor (Fan et al., 2001; Liu et al., 2005a,b; Kafi et al., 2007). A number of biosensors have been fabricated based on horseradish peroxidase (HRP) using various different methods (Zhao et al., 2004; Yu et al., 2005; Sun et al., 1998; Liu et al., 2005a,b). HRP is a heme enzyme with a molar weight of ~44 kDa, which is able to catalyze the oxidation of a wide variety of substrates by $H_2O_2$. In addition, it has been demonstrated that the reduced form of HRP can be reoxidized chemically by $H_2O_2$ (Liu et al., 2005a,b).

When immobilizing enzymes or proteins on solid substrates, it is important to keep high electroactivity of the protein or enzyme immobilized on the electrode surface as unfavorable orientation or direct adsorption of biomolecules onto a metal electrode surface may dramatically lower their catalytic activity (Zhang and Li, 2004). The performance of a biosensor mainly depends on the properties of the bioactive layer associated with the transducer (Girard-Egrot et al., 2003). In order to retain its high electroactivity, different matrices have been used for the immobilization of HRP (Chattopadhyay and Mazumdar, 2000; Setti et al., 2007; Yu and Ju, 2002; Kong et al., 2003). Among these, inorganic nanostructured materials are more promising because of their regular structure, high active surface area for protein binding, and good chemical and thermal stability (Wang et al., 2003). Since the discovery of carbon nanotubes, increasing attention has been paid to the study of one-dimensional nanostructures such as nanotubes, nanorods

* Corresponding author. Tel.: +1 807 3438318; fax: +1 807 3467775.
*E-mail address:* aicheng.chen@lakeheadu.ca (A. Chen).

0956-5663/$ – see front matter © 2008 Elsevier B.V. All rights reserved.
doi:10.1016/j.bios.2008.06.004

and nanowires. Titanium dioxide ($TiO_2$) can be formed into different morphologies such as nanoparticles, nanofibres, nanotubes and nanosheets (Peng and Chen, 2006; Ou and Lo, 2007). $TiO_2$ nanotubes are very good biocompatible inorganic material, inexpensive, environmentally benign, and chemically and thermally stable (Tremel, 1999). $TiO_2$ nanotube arrays have demonstrated a number of important applications including gas sensing, solar cells, photocatalysts, tissue engineering and biosensors (Liu et al., 2005a,b; Yoriya et al., 2007). Our recent study has shown that $TiO_2$ nanotubes with large surface areas and good uniformity and conformability over large areas fabricated by the anodic oxidation of Ti substrates are very promising for the immobilization of biomolecules for electrochemical biosensor design (Liu and Chen, 2005).

In this paper, for the first time, we report on a promising $H_2O_2$ biosensor based on the co-immobilization of HRP and chitosan onto Au-modified titanium dioxide nanotube arrays. The $TiO_2$ nanotube arrays were synthesized by anodizing Ti substrates in an electrolyte of dimethyl sulfoxide (DMSO) containing hydrofluoric acid (2% HF) first. Then an Au thin film was uniformly coated on the $TiO_2$ nanotube arrays using a plasma sputtering technique. Our electrochemical measurements reveal that the immobilized HRP exhibits high biological activity and stability. The amperometric response of the developed biosensor to $H_2O_2$ concentration has long-range linearity. In addition, our study demonstrates that the presence of methylene blue (MB) further enhances the sensitivity of the designed $H_2O_2$ electrochemical biosensor.

## 2. Experimental

### 2.1. Reagents and materials

HRP (EC1.11.1.7, Type X) was purchased from Sigma, used as received and stored at 4 °C. MB was obtained from the British Drug Houses Ltd., Poole, England; chitosan was from Aldrich. 30% hydrogen peroxide was bought from Fluka and the stock solution of $H_2O_2$ was diluted from this. Hydrofluoric acid (HF, 49%) came from Fisher chemical and DMSO from Caledon Laboratories Ltd., Canada. All experimental solutions were prepared every day by appropriate dilution of the stock solutions. All other reagents were of analytical grade and used as supplied. The pure water (18 MΩ cm) used to prepare all solutions in this study was purified with the Nanopure® water system. All experiments were performed in 0.1 mol $l^{-1}$ phosphate buffer solutions (PBS) whose pH values were adjusted with $K_2HPO_4$ and $KH_2PO_4$.

### 2.2. Biosensor fabrication

The $TiO_2$ nanotubes were directly grown on Ti substrates by a facile anodic oxidation method which has been described previously (Yoriya et al., 2007; Tian et al., 2008). Briefly, pure titanium foils were ultrasonically cleaned in acetone and ethanol prior to anodization. After rinsing with distilled water, a clean titanium foil (0.8 cm × 1.0 cm × 0.05 cm) was first etched in an 18% HCl solution at 85 °C for 10 min. The etched titanium foil was rinsed thoroughly with pure water and then anodized in a two-electrode electrochemical cell in an electrolyte containing DMSO and hydrofluoric acid (HF, 2%) at 40 V for 8 h. A platinum coil was used as the counter electrode. After the anodization, samples were rinsed thoroughly with pure water and then ultrasonicated to remove surface debris. In order to improve the crystalline properties and remove the remnants, the anodized samples were annealed at 450 °C for 1 h under ambient atmosphere. The Au thin film was then coated onto the $TiO_2$ nanotube arrays by argon plasma sputtering for 30 s. Finally, 20 μl of 2 mg/ml of HRP and 10 μl of 2 mg/ml of chitosan were co-immobilized onto the synthesized Au-coated $TiO_2$ nanotube arrays ($Ti/TiO_2/Au/HRP$). For comparison, a $H_2O_2$ biosensor based on the $TiO_2$ nanotube arrays without the Au thin film ($Ti/TiO_2/HRP$) was also fabricated in the same way. The resulting electrodes were stored in 0.1 mol $l^{-1}$ PBS at pH 7.0 and 4 °C when not being in use.

### 2.3. Surface characterization and electrochemical measurements

Electrochemical measurements were carried out with a CHI (630B) workstation. A three-electrode configuration was employed in this study. The fabricated $Ti/TiO_2/Au/HRP$ and $Ti/TiO_2/HRP$ biosensors were employed as the working electrodes. A platinum coil was used as the counter electrode, and a KCl saturated Ag/AgCl electrode was used as the reference electrode. For cyclic voltammetry the working electrode was cycled in a 0.1 mol $l^{-1}$ PB solution by applying voltage in the range between 0.0 and −0.8 V versus Ag/AgCl. Amperometric measurements were carried out in a stirred cell by applying a potential of −0.6 V to the working electrode. A magnetic stirrer was used for this experiment. All electrolytes were deoxygenated by bubbling ultra-pure argon for 30 min prior to the experiment and maintained under argon atmosphere during the course of the experiment. All measurements were performed at room temperature.

The morphology and composition of the synthesized $TiO_2$ nanotube arrays were characterized by scanning electron microscope (SEM) (JEOL JSM 5900 LV) at an acceleration voltage of 13 kV and an energy-dispersive X-ray (EDX) spectrometer.

## 3. Results and discussion

### 3.1. Surface characterization of the Au-modified $TiO_2$ nanotube arrays

The morphology and composition of the Ti substrate after the anodization and the Au coating were examined by SEM observation and EDS analysis. Fig. 1a presents the SEM image of the $TiO_2$ nanotube arrays directly grown on a Ti substrate by anodizing the Ti substrate in an electrolyte containing DMSO and hydrofluoric acid (HF, 2%) at 40 V for 8 h. All the nanotubes have a unique open-mouth structure on the top of the $TiO_2$ layer. The estimated dimensions of the formed $TiO_2$ nanotubes are ~100 nm in outer diameter, ~80 nm in inner diameter and ~20 nm of wall-thickness. After coating a gold thin film onto the $TiO_2$ nanotube arrays by argon plasma sputtering for 30 s, as expected, the surface morphology of the Au-coated $TiO_2$ nanotube arrays is exactly the same as shown in Fig. 1a. However, in addition to the O and Ti peaks observed in the EDS spectrum of the $TiO_2$ nanotube arrays, a strong Au peak appears in the EDS spectrum of the Au-coated $TiO_2$ nanotube arrays as shown in Fig. 1b. Further quantitative analysis reveals that the ratio of Ti to O is closed to 1:2, confirming that the formed nanotubes are $TiO_2$. The high adhesion and integrity of the synthesized $TiO_2$ nanotube layer are important for the immobilization of biomolecules. The $TiO_2$ layer directly grown on the Ti substrate using the anodization method has much better adhesion to the Ti substrate than others which are synthesized by other methods first, and then immobilized on an electrode surface (Xiao et al., 2007). Since the $TiO_2$ nanotube arrays are directly grown from the Ti substrate, and by taking into all other considerations such as non-toxicity, high surface area, and the strong thermal and chemical stability of $TiO_2$ nanotubes, it is expected that the Au-modified $TiO_2$ nanotube arrays synthesized in this study are desirable for biosensing applications.

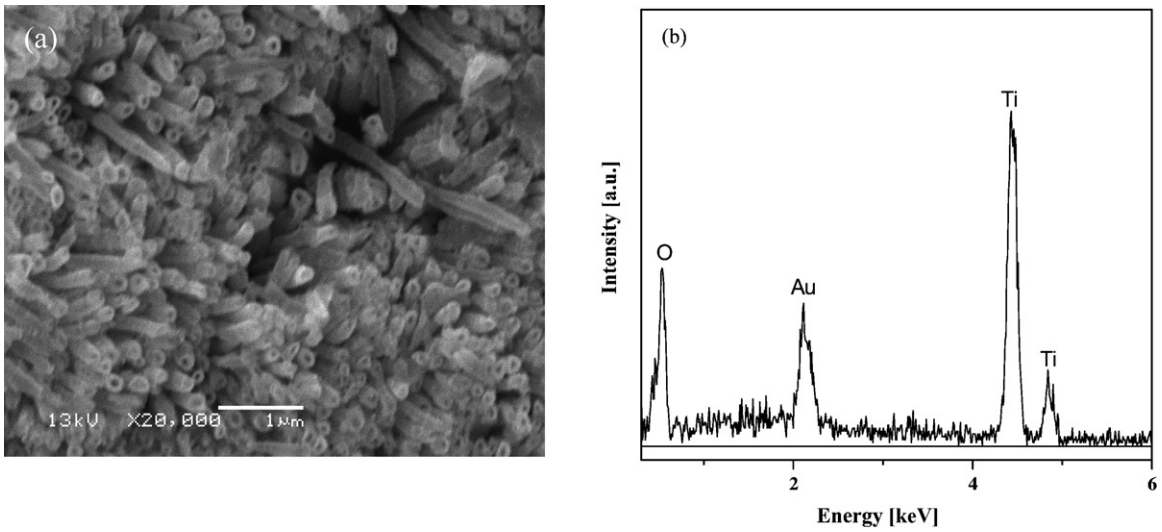


**Fig. 1.** (a) SEM image of the $TiO_2$ nanotube arrays grown on Ti substrate; (b) EDS spectrum of the Au-modified $TiO_2$ nanotube arrays.

### 3.2. Direct electrochemistry

Fig. 2a compares the cyclic voltammograms (CVs) of the Ti/$TiO_2$ (dashed line) and Ti/$TiO_2$/Au (solid line) electrodes recorded in a 0.1 mol $l^{-1}$ KCl + $5.0 \times 10^{-3}$ mol $l^{-1}$ $Fe(CN)_6^{3-/4-}$ solution at a sweep rate of 50 mV/s. $TiO_2$ is a semiconductor and its electrical conductivity is relatively low. As expected, neither oxidation nor reduction peak is observed in the CV of the Ti/$TiO_2$ electrode. In contrast, a well-defined and large pair of oxidation peaks located at 0.32 V and a reduction peak centered at 0.09 V appear in the CV of the Ti/$TiO_2$/Au electrode. The above results show that the presence of the Au thin film significantly increases the electrical activity of the $TiO_2$ nanotube arrays.

Fig. 2b presents the three cyclic voltammograms of the Ti/$TiO_2$ (dotted line), Ti/$TiO_2$/HRP (dashed line) and Ti/$TiO_2$/Au/HRP electrode (solid line) recorded in 0.1 mol $l^{-1}$ PBS (pH 7.0) at the sweep rate of 50 mV/s. The CVs of both Ti/$TiO_2$/Au and Ti/$TiO_2$/Au/HRP electrodes are flat and no obvious corresponding peak is observed. However, a pair of small redox peaks appear in the CV of the Ti/$TiO_2$/Au/HRP electrode (solid line the anodic and cathodic peak potentials are located at about −0.39 and −0.47 V, respectively. The formal potential $E_0$ was calculated to be −0.43 V. We further investigated the effect of the scanning rates on the response of the Ti/$TiO_2$/Au/HRP electrode. Our results show (data not shown here), with the increase of the scan rates from 50 to 500 mV/s, the redox peak current increases linearly. The peak-to-peak separation also increases with the increase of the scan rates. All the above experimental results show that: (i) the redox peak arises from the electrochemical reaction of the immobilized HRP; (ii) this redox process is quite quasi-reversible and surface-controlled; (iii) direct electron transfer occurs between the immobilized HRP and the Ti/$TiO_2$/Au electrode; (iv) the coated Au thin film plays a key role in enhancing the electron transfer; (v) the Au-coated $TiO_2$ nanotube arrays provide a good matrix for HRP immobilization and biosensor fabrication.

### 3.3. Electrochemical response of the Ti/$TiO_2$/Au/HRP biosensor to $H_2O_2$

Fig. 3 shows typical CVs of the Ti/$TiO_2$/Au/HRP electrode recorded in the absence and presence of $3.0 \times 10^{-3}$ mol $l^{-1}$ $H_2O_2$ in 0.1 mol $l^{-1}$ PBS at pH 7.0 with or without the addition of MB at a scan rate of 50 mV/s. In the absence of $H_2O_2$, a pair of small redox peaks due to the direct electron transfer between the immobilized

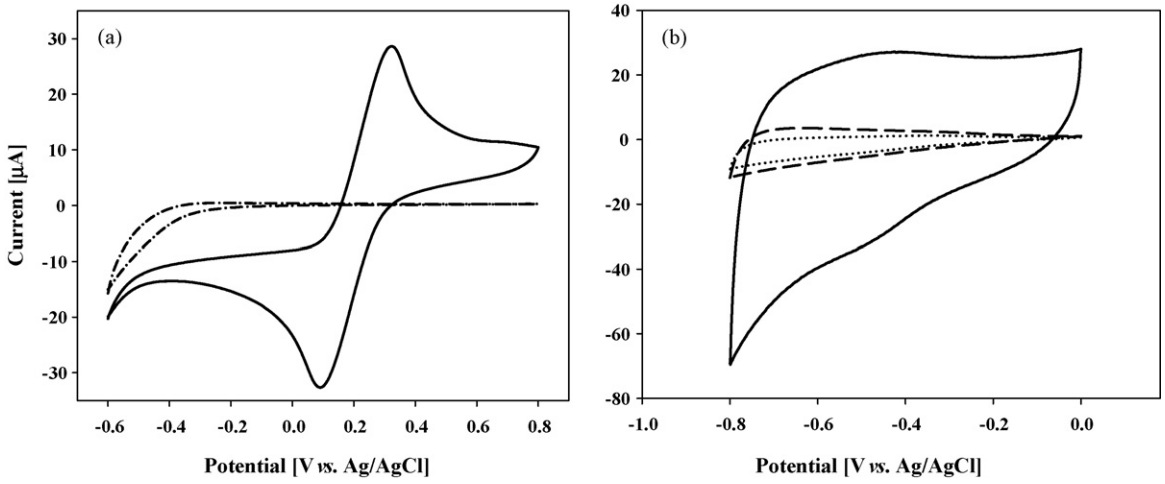


**Fig. 2.** (a) Cyclic voltammamograms response at Ti/$TiO_2$ (dashed line) and Ti/$TiO_2$/Au (solid line) electrodes in $5 \times 10^{-3}$ mol $l^{-1}$ $Fe(CN)_6^{3-/4-}$ and 0.1 mol $l^{-1}$ KCl solution; (b) cyclic voltammamograms of Ti/$TiO_2$/Au/HRP electrode (solid line), Ti/$TiO_2$/HRP (dashed) and Ti/$TiO_2$ (dotted) in 0.1 mol $l^{-1}$ PBS at pH 7.0 at a scan rate of 50 mV/s.

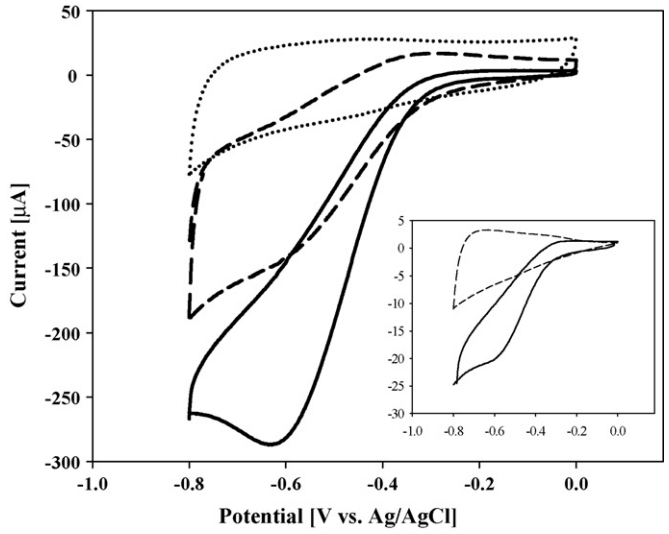


**Fig. 3.** Cyclic voltammamograms of $Ti/TiO_2/Au/HRP$ electrode in the absence and presence of $3 \times 10^{-3}$ mol $l^{-1}$ $H_2O_2$ in 0.1 mol $l^{-1}$ PBS at pH 7.0 at a scan rate of 50 mV/s (dotted line: blank solution; dashed line: $3 \times 10^{-3}$ mol $l^{-1}$ $H_2O_2$ with no MB; solid line: $3 \times 10^{-3}$ mol $l^{-1}$ $H_2O_2$ in the presence of $1.1 \times 10^{-3}$ mol $l^{-1}$ of MB). The inset shows the CVs of $Ti/TiO_2/HRP$ in the absence (dashed line) and presence (solid line) of $3 \times 10^{-3}$ mol $l^{-1}$ $H_2O_2$ in 0.1 mol $l^{-1}$ PBS in the absence of MB at pH 7.0 at a scan rate of 50 mV/s.

HRP and the $Ti/TiO_2/Au$ electrode appears in the CV (dotted line), similar to the observation in Fig. 2b. When $3.0 \times 10^{-3}$ mol $l^{-1}$ $H_2O_2$ was added to the electrolyte (dashed line), the reduction peak current on the $Ti/TiO_2/Au/HRP$ electrode increased, accompanied by a decrease of the oxidation peak current. However, no similar phenomenon was found at the $Ti/TiO_2$ electrode (data not shown here), showing that the catalytic reduction of $H_2O_2$ indeed originates from the immobilized HRP. For comparison, we also recorded two CVs of the $Ti/TiO_2/HRP$ electrode in the absence of (dashed line) and in the presence of $3.0 \times 10^{-3}$ mol $l^{-1}$ $H_2O_2$ (solid line) in 0.1 mol $l^{-1}$ PBS at pH 7.0 at a scan rate of 50 mV/s as shown in the inset of Fig. 3. The catalytic reduction current of $H_2O_2$ at the $Ti/TiO_2/HRP$ electrode is much smaller than that at the $Ti/TiO_2/Au/HRP$ electrode, indicating that the coated Au thin film greatly enhances the catalytic activity of the immobilized HRP and that the HRP immobilized onto $TiO_2$ nanotube arrays retains its bioactivity. The catalytic mechanism of the immobilized HRP to $H_2O_2$ reduction can be explained by the following scheme (Yi et al., 2000):

$$HRP(Fe^{3+}) + H_2O_2 \rightarrow CompoundI(Fe^{4+} = O) + H_2O \quad (1)$$

$$CompoundI(Fe^{4+} = O) + e^- + H^+ \rightarrow CompoundII \quad (2)$$

$$CompoundII + e^- + H^+ \rightarrow HRP(Fe^{3+}) + H_2O \quad (3)$$

HRP reacts with $H_2O_2$ to form the intermediate (Compound I), which is a two-equivalent oxidized form containing oxyferryl heme and a porphyrin π cation radical. Compound I has catalytic activity and its porphyrin radical gains one electron from the electrode to form another intermediate (Compound II), which is subsequently reduced back to the native HRP by accepting another electron from the electrode.

To further improve the sensitivity of the proposed $H_2O_2$ biosensor, MB was added and used as an electron mediator. In Fig. 3, the solid line represents the CV of the $Ti/TiO_2/Au/HRP$ electrode recorded in 0.1 mol $l^{-1}$ PBS at pH 7.0 containing $1.1 \times 10^{-3}$ mol $l^{-1}$ MB and $3.0 \times 10^{-3}$ mol $l^{-1}$ $H_2O_2$ at a scan rate of 50 mV/s. The catalytic peak current for $H_2O_2$ reduction at the $Ti/TiO_2/Au/HRP$ electrode in the presence of MB in the electrolyte is over 120% higher than that in the absence of MB (dashed line), showing that MB plays an important role as an electron mediator and that the presence of MB greatly improves the sensitivity of the proposed biosensor. The significant increase of the sensitivity by MB can be illustrated by the following possible reaction mechanism (Chen et al., 2006):

$$HRP(red) + H_2O_2 \rightarrow HRP(ox) + H_2O \quad (4)$$

$$HRP(ox) + MB(red) \rightarrow HRP(red) + MB(ox) \quad (5)$$

$$MB(ox) + e^- \rightarrow MB(red) \quad (6)$$

Firstly, hydrogen peroxide in the electrolyte is reduced by the HRP (red), forming HRP (ox). Secondly, HRP (red) can be regenerated with the help of the mediator MB, while the MB (red) is oxidized in the enzymatic reaction. Finally, the MB (ox) is electrochemically reduced on the electrode surface. MB is an electron mediator and it accelerates electron transfer, leading to the great increase of the reduction current.

### 3.4. Optimization of experimental parameters

It is well known that the applied potential strongly affects the amperometric response of a biosensor. We have systemically investigated the impact of applied potentials on the amperometric response of the $Ti/TiO_2/Au/HRP$ electrode to $H_2O_2$. Fig. 4a shows the current response at different applied potentials in the presence of $3.0 \times 10^{-5}$ mol $l^{-1}$ $H_2O_2$ in a 0.1 mol $l^{-1}$ PBS (pH 7.0) containing $1.1 \times 10^{-3}$ mol $l^{-1}$ of MB. The steady-state reduction current increases gradually as the applied electrode potential decreases from −0.1 to −0.6 V. The maximum reduction current was achieved at around −0.6 V. At more negative potentials, there may be interfering reactions from other electroactive species in the solution.

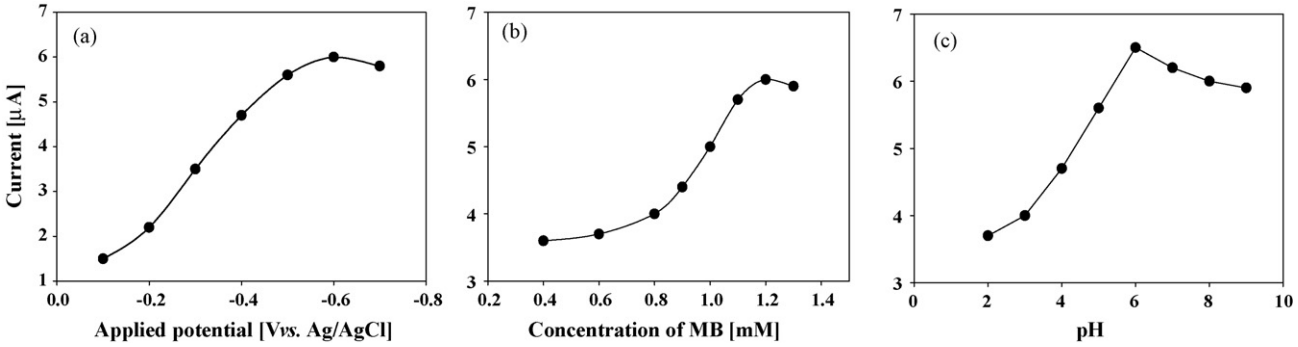


**Fig. 4.** (a) Dependence of catalytic current of the biosensor at different applied potentials measured in a pH 7.0 PBS containing $3 \times 10^{-5}$ mol $l^{-1}$ $H_2O_2$ and $1.1 \times 10^{-3}$ mol $l^{-1}$ of MB; (b) effect of the MB concentration on the amperometric response of the $Ti/TiO_2/Au/HRP$ electrode to $3 \times 10^{-5}$ mol $l^{-1}$ of $H_2O_2$ in PBS (pH 7.0) at the potential of −0.6 V; (c) influence of pH on the catalytic current of the biosensor in the presence of $3 \times 10^{-5}$ mol $l^{-1}$ $H_2O_2$ in PBS containing $1.2 \times 10^{-3}$ mol $l^{-1}$ of MB at the potential of −0.6 V.

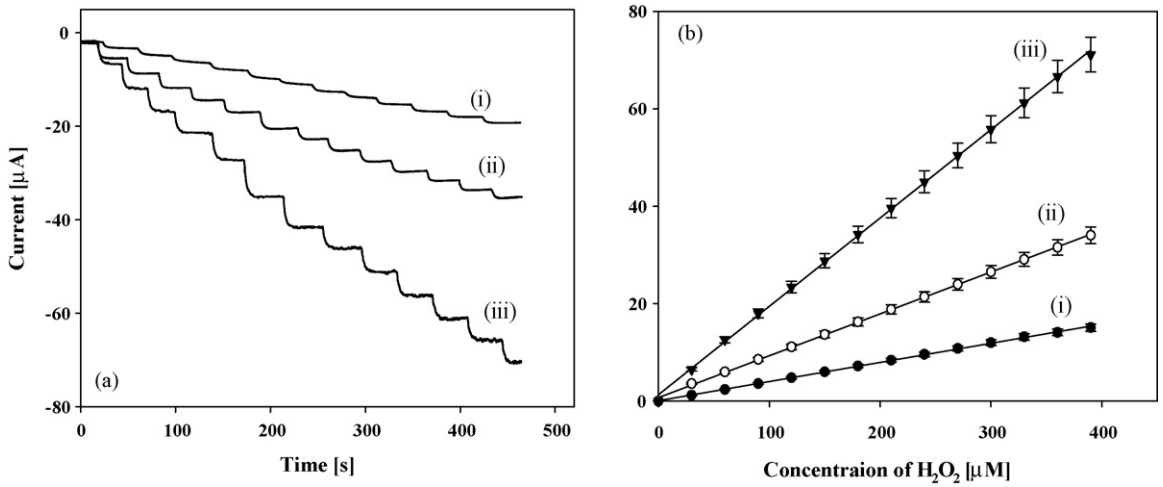


**Fig. 5.** (a) Typical amperometric response of the Ti/$TiO_2$/HRP electrode without the addition of MB (i), the Ti/$TiO_2$/Au/HRP biosensor in the absence of MB (ii) and in the presence of $1.2 \times 10^{-3}$ mol $l^{-1}$ MB (iii) with total additions of $3.9 \times 10^{-4}$ mol $l^{-1}$ $H_2O_2$ in 0.1 mol $l^{-1}$ PBS (pH 6.0) at the operating potential of −0.6 V. (b) Calibration plots for the Ti/$TiO_2$/HRP electrode and the proposed Ti/$TiO_2$/Au/HRP biosensor (the same experimental conditions as Fig. 5a).

Therefore, we chose the applied potential of −0.6 V as the working potential for this proposed biosensor, where the background current is minimized and unexpected interfering reactions of the other electroactive species can be avoided effectively.

As shown in Fig. 3, the presence of MB greatly increases the $H_2O_2$ reduction current. To optimize the amount of the mediator, we further studied the influence of MB concentration on the Ti/$TiO_2$/Au/HRP electrode for $H_2O_2$ detection. Fig. 4b shows the amperometric response of the Ti/$TiO_2$/Au/HRP electrode to $3 \times 10^{-5}$ mol $l^{-1}$ of $H_2O_2$ in 0.1 mol $l^{-1}$ PBS (pH 7.0) at the potential of −0.6 V versus the MB concentration, where the concentration of MB varies from $4.0 \times 10^{-4}$ to $1.3 \times 10^{-3}$ mol $l^{-1}$. It is noteworthy that when the concentration of MB is higher than $1.2 \times 10^{-3}$ mol $l^{-1}$, instead of increasing, the current response slightly decreases. The maximum current response was achieved in the presence of $1.2 \times 10^{-3}$ mol $l^{-1}$ MB. At the low or very high concentration of MB, the amperometric response could be limited by enzyme-mediator kinetics (Xiao et al., 1999). At the high concentration of MB, an unexpected background current could also be produced or MB can be adsorbed on the electrode surface, which may result in the decrease of the sensitivity of the biosensor (Lei et al., 2004). To achieve the highest sensitivity and to avoid the extra background current, $1.2 \times 10^{-3}$ mol $l^{-1}$ of MB was thus chosen for the following experiments.

The performance of a biosensor also strongly depends on the pH value of electrolytes. Fig. 4c presents the amperometric response of the Ti/$TiO_2$/Au/HRP electrode at different pH in the presence of $3 \times 10^{-5}$ mol $l^{-1}$ of $H_2O_2$ and $1.2 \times 10^{-3}$ mol $l^{-1}$ of MB. The steady-state current is increased with the increasing of the pH from 3.0 to 6.0; however, the amperometric response decreases when the pH further increases from 7.0 to 9.0. At the lower pH values (<4.0), the current response is very low, which might be due to the denaturation of biomolecules (Chen et al., 1999). The pH range of 6.0–7.5 reflects the optimum conditions for enzymatic mediated electrochemical reactions (Santos et al., 2007). As the maximum amperometric response is achieved at pH 6.0, this pH is considered as the optimized pH for the proposed Ti/$TiO_2$/Au/HRP biosensor.

We further investigated the effect of the anodization time of the Ti substrate on the sensitivity of the biosensor. The amperometric response increases with the increment of the anodization time from 0 to 8 h (data not shown here). This is consistent with the increase of the length of the formed $TiO_2$ nanotubes and the active surface area of the formed $TiO_2$ nanotube arrays when the anodic oxidation time increases from 2 h, when the tubes begin to appear, to 8 h. However, when we further increase the anodization time, the amperometric response of the biosensor slightly decreases. 8 h is thus considered as the optimized anodization time.

### 3.5. Amperometric response and stability of the biosensor

The amperometric response of the Ti/$TiO_2$/Au/HRP biosensor was tested in a stirred cell containing 0.1 mol $l^{-1}$ PBS (pH 6.0) under the optimized operating electrode potential of −0.6 V. For comparison, Fig. 5a presents the typical amperometric response of the Ti/$TiO_2$/HRP electrode without the addition of MB (i); the Ti/$TiO_2$/Au/HRP biosensor in the absence of MB (ii); in the presence of $1.2 \times 10^{-3}$ mol $l^{-1}$ MB (iii), for successive additions of $H_2O_2$. The corresponding calibration plots for the three amperometric

**Table 1**
Comparison of the performance of different $H_2O_2$ biosensors (HRP = horseradish peroxidase; Hb = hemoglobin; LOD = limit of detection)

| Electrode | LOD (μM) | Stability | Reference |
|---|---|---|---|
| Hb in $TiO_2$ nanotube | 4.6 | 90% (21 days) | Zheng et al. (2008) |
| Hb in Au-nanoparticle | 4.5 | 95% (40 days) | Zhang and Oyama (2004) |
| Hb in carbon nanotube | 9.0 | Not reported | Zhao et al. (2005) |
| HRP in nano-Au on Pt electrode | 0.17 | 84.2% (30 days) | Cao et al. (2007) |
| HRP in nano-Au with sol–gel | 6.1 | 75% (35 days) | Lei et al. (2004) |
| HRP in nano-Au on GC electrode | 0.64 | 70% (30 days) | Gao et al. (2007) |
| HRP in nano-Au with sol–gel | 6.1 | 75% (35 days) | Lei et al. (2004) |
| HRP in SAM-nano-Au | 0.5 | 97.4% (7 days) | Xu et al. (2007) |
| HRP in carbon nanotube | 12.89 | Not reported | Chen and Dong (2007) |
| Proposed biosensor | 2 | 95% (21 days) | |

response curves are shown in Fig. 5b. The amperometric response of the $Ti/TiO_2$/Au/HRP hydrogen peroxide biosensor is much higher than that of the $Ti/TiO_2$/HRP electrode. The presence of MB further increases the response of the $Ti/TiO_2$/Au/HRP biosensor. As seen in curve (iii), in the presence of MB, the response of the $Ti/TiO_2$/Au/HRP biosensor is very quick; over 95% of the steady-state current is achieved within 5 s. Under the optimized experimental parameters, the developed $Ti/TiO_2$/Au/HRP biosensor shows a linear response within the range of $5 \times 10^{-6}$ to $4 \times 10^{-4}$ mol $l^{-1}$ concentrations of $H_2O_2$ with a correlation coefficient of 0.996. The detection limit was determined to be $2 \times 10^{-6}$ mol $l^{-1}$ (based on the S/N = 3).

The long-term stability of this biosensor was also investigated. The $Ti/TiO_2$/Au/HRP electrode was stored in PBS (pH 7.0) at 4 °C when not being in use. It retained 95% of its initial current response after 21 days. The repeatability of the sensor for current response was also examined. It was found that the relative standard deviation (R.S.D.) was 3.75% for 10 successive measurements at a $H_2O_2$ concentration of $3 \times 10^{-5}$ mol $l^{-1}$. The performance of the $Ti/TiO_2$/Au/HRP biosensor developed in this study was compared with other biosensors as shown in Table 1, showing that our proposed biosensor shows excellent performance in terms of low detection limit and high stability.

## 4. Conclusions

In this paper, we have demonstrated a promising $H_2O_2$ biosensor based on the co-immobilization of HRP and chitosan onto Au-modified titanium dioxide nanotube arrays. The titania nanotube arrays were directly grown on a titanium substrate by simple anodic oxidation. These titania nanotube arrays possess large surface area and good uniformity, providing an excellent matrix for the co-immobilization of HRP and chitosan. The presence of the Au thin film greatly increases the electrical activity of the formed $TiO_2$ nanotube arrays. Our electrochemical measurements reveal that the immobilized HRP exhibits high biological activity and stability. The amperometric response of the developed biosensor to $H_2O_2$ concentration has long-range linearity. In addition, our study demonstrates that the presence of MB further enhances the sensitivity of the designed $H_2O_2$ electrochemical biosensor. Under optimal conditions, the designed biosensor exhibits fast amperometric response, excellent linear relationships, and a low detection limit. In addition, it shows very high sensitivity, good reproducibility and long-time stability. In summary, ease of fabrication, a low cost, fast response and high sensitivity make the biosensor proposed in this study very promising in the pharmaceutical, clinical and industrial detection of $H_2O_2$.

## Acknowledgments

This work was supported by a Discovery Grant from the Natural Sciences and Engineering Research Council of Canada (NSERC). A.K.M. Kafi acknowledges the Ontario Post Doctoral Fellowship.

## References

Cao, S., Yuan, R., Chai, Y., Zhang, L., Li, X., Gao, F., 2007. Bioprocess. Biosyst. Eng. 30, 71–78.
Chattopadhyay, K., Mazumdar, S., 2000. Bioelectrochemistry 53, 17–24.
Chen, H., Dong, S., 2007. Biosens. Bioelectron. 22, 1811–1815.
Chen, X., Hu, N., Zeng, Y., Rusling, J.F., Yang, J., 1999. Langmuir 15, 7022–7030.
Chen, S., Yuan, R., Chai, Y., Xu, L., Wang, N., Li, X., Zhang, L., 2006. Electroanalysis 18, 471–477.
Clark, L.C., Lyons, C., 1962. Ann. N.Y. Acad. Sci. 102, 29–45.
Fan, C., Wang, H., Sun, S., Zhu, D., Wagner, G., Li, G., 2001. Anal. Chem. 73, 2850–2854.
Ferapontova, E.E., Grigorenko, V., Egorov, A.M., Borchers, T., Ruzgas, T., Gorton, L., 2001. Biosens. Bioelectron. 16, 147–157.
Gao, F., Yuan, R., Chai, Y., Chen, S., Cao, S., Tang, M., 2007. J. Biochem. Biophys. Methods 70, 407–413.
Girard-Egrot, A.P., Godoy, S., Chauvet, J.P., Boullanger, P., Coulet, P.R., 2003. Biochim. Biophys. Acta 1617, 39–51.
Hurdis, E.C., 1954. Anal. Chem. 26, 320–325.
Jia, W.-Z., Hu, Y.-L., Song, Y.-Y., Wang, K., Xia, X.-H., 2008. Biosens. Bioelectron. 23, 892–898.
Kafi, A.K.M., Lee, D.Y., Park, S.H., Kwon, Y.S., 2007. J. Nanosci. Nanotechnol. 7, 4005–4008.
Kim, Y.-P., Oh, Y.-H., Kim, H.-S., 2008. Biosens. Bioelectron. 23, 980–986.
Kong, Y.T., Boopathi, M., Shim, Y.B., 2003. Biosens. Bioelectron. 19, 227–232.
Lei, C.X., Hu, S.Q., Gao, N., Shen, G.L., Yu, R.Q., 2004. Bioelectrochemistry 65, 33–39.
Li, J., Dasgupta, P.K., 2000. Anal. Chem. 72, 5338–5347.
Liu, S., Chen, A., 2005. Langmuir 21, 409–8413.
Liu, S., Miller, B., Chen, A., 2005a. Electrochem. Commun. 7, 1232–1236.
Liu, Z.M., Yang, Y., Wang, H., Liu, Y.L., Shen, G.L., Yu, R.Q., 2005b. Sens. Actuator B 106, 394–400.
Matsubara, C., Kawamoto, N., Takamura, K., 1992. Analyst 117, 1781–1784.
Nakashima, K., Maki, K., Kawaguchi, S., Akiyama, S., Tsukamoto, Y., Kazuhiro, I., 1991. Anal. Sci. 7, 709–714.
Ou, H.H., Lo, S.L., 2007. Sep. Purif. Technol. 58, 179–191.
Peng, X., Chen, A., 2006. Adv. Funct. Mater. 16, 1355–1362.
Santos, A.S., Pereira, A.C., Sotomayor, M.D.P.T., Tarley, C.R.T., Duran, N., Kubota, L.T., 2007. Electroanalysis 19, 549–554.
Setti, L., Fraleoni-Morgera, A., Mencarelli, I., Filippini, A., Ballarin, B., Di Biase, D., 2007. Sens. Actuator B 126, 252–257.
Shumyantseva, V.V., Ivanov, Y.D., Bistolas, N.F., Scheller, W., Archakov, A.I., Wollenberger, U., 2004. Anal. Chem. 76, 6046–6052.
Sun, J.J., Fang, H.Q., Cheng, H.Y., 1998. Analyst 123, 1365–1368.
Sun, Y.X., Zhang, J.T., Huang, S.W., Wang, S.F., 2007. Sens. Actuator B 124, 494–500.
Tian, M., Wu, G., Adams, B., Wen, J., Chen, A., 2008. J. Phys. Chem. C 112, 825–831.
Tremel, W., 1999. Angew. Chem. Int. Ed. 38, 2175–2179.
Wang, L., Wang, E., 2004. Electrochem. Commun. 6, 225–229.
Wang, J., Musameh, M., Lin, Y., 2003. J. Am. Chem. Soc. 125, 2408–2409.
Xiao, X.F., Tian, T., Liu, R.F., She, H.D., 2007. Mater. Chem. Phys. 106, 27–32.
Xiao, Y., Ju, H.X., Chen, H.Y., 1999. Anal. Chim. Acta 391, 73–82.
Xu, S., Peng, B., Han, X., 2007. Biosens. Bioelectron. 22, 1807–1810.
Yi, X., Ju, H.X., Chen, H.Y., 2000. Anal. Biochem. 278, 22–28.
Yoriya, S., Paulose, M., Varghese, O.K., Mor, G.K., Grimes, C.A., 2007. J. Phys. Chem. C 111, 13770–13777.
Yu, J.H., Ju, H.X., 2002. Anal. Chem. 74, 3579–3583.
Yu, P., Lin, Y., Xiang, L., Su, L., Zhang, J., Mao, L., 2005. Langmuir 21, 9000–9006.
Zhang, W.J., Li, G.X., 2004. Anal. Sci. 20, 603–610.
Zhang, J., Oyama, M., 2004. Electrochim. Acta 50, 85–90.
Zhao, F., Wu, X., Wang, M., Liu, Y., Gao, L., Dong, S., 2004. Anal. Chem. 76, 4960–4967.
Zhao, Y.D., Bi, Y.H., Zhang, W.D., Luo, Q.M., 2005. Talanta 65, 489–494.
Zheng, W., Zheng, Y.F., Jin, K.W., Wang, N., 2008. Talanta 74, 1414–1419.